Engineering Structures 111 (2016) 80–92

Contents lists available at ScienceDirect

Engineering Structures

journal homepage: www.elsevier.com/locate/engstruct

Experimental study on the progressive collapse performance of RC frames with infill walls

Sidi Shan [a,b], Shuang Li [a,b,*], Shiyu Xu [c], Lili Xie [b,d]

[a] Key Lab of Structures Dynamic Behavior and Control of the Ministry of Education (Harbin Institute of Technology), Harbin 150090, China
[b] School of Civil Engineering, Harbin Institute of Technology, Harbin 150090, China
[c] Department of Architecture and Civil Engineering, City University of Hong Kong, Hong Kong Special Administrative Region
[d] Institute of Engineering Mechanics, China Earthquake Administration, Heilongjiang, Harbin 150080, China

ARTICLE INFO

Article history:
Received 28 January 2015
Revised 1 December 2015
Accepted 13 December 2015
Available online 6 January 2016

Keywords:
Reinforced concrete frame
Progressive collapse performance
Experiment
Infill wall
Failure mode

ABSTRACT

The interaction between the infill walls and the reinforced concrete (RC) frame members in the progressive collapse process was examined experimentally in this study. Two 1/3 scaled, four-bay, two-story RC frame specimens, one of which was featured without infill walls while the other with infill walls, were tested. The frame specimens were designed in such a way that the center column of the first story was missing, in order to simulate the failure of the structural component due to abnormal loads or design flaws. The frame specimens were quasi-statically pushed downward at the top of center column under displacement control to investigate the progressive collapse mechanism of the RC frames, with a focus on the effects of infill walls. Specifically, the physical quantities and phenomena of great interest in this study include the collapse resistance force and mechanism, strain variation and crack development in structural components, and local and global failure modes of the frames. The test results showed that the infill walls can provide alternative load paths for transferring the loads originally only supported by the beams, and thus, improve the collapse resistance capacity of the RC frame. The infill walls, however, may reduce the ductility of the RC frame and may change the failure mode of the frame. It is concluded that the infill walls may affect (i.e., either improve or impair) the performance of RC frames against progressive collapse in different aspects.

1. Introduction

In present design practice, the structural members of buildings normally are proportioned according to the strength and displacement demands imposed on the structures when the structures are subjected to various load combinations (known as the *limit states*), considering the regular dead loads and live loads such as the gravitational load, seismic load, and wind load, etc. However, when the exceptionally large-magnitude, unpredicted loads are applied to a certain portion of these kinds of code-conforming buildings, progressive collapse may still occur. Progressive collapse is the phenomenon of disproportionate damage to structures, initiated by the loss of local members which can be induced by abnormal loads, design flaws or malevolent events. Famous progressive collapse events includes the collapse of Ronan Point building in 1968 due to gas explosion and the collapses of Murrah Federal Building and World Trade Center in 1995 and 2001, respectively, owing to the terrorist attack [1]. It is generally recognized that the main resisting mechanism with respect to progressive collapse of frame structures include flexural action [2], compressive arch action and catenary action [3,4]. Flexural action is the resistance forces provided by flexural resistance of frame members. Compressive arch action refer to the compressive arch formed in beams due to the restraint of surrounding columns. Catenary action is the vertical resistance mobilized by axial tension force developed in beams at large displacements. Despite the fact that infill walls are commonly considered as non-structural members, it is well known that the infill walls behave as struts (often used in numerical models for seismic analysis) in frame structures and may have non-negligible effects on a structure's resistance capacity against various failure modes. Nonetheless, although many experimental and numerical studies on progressive collapse of RC frame structures [5–14] have been performed, very few of them have taken the interaction between the infill walls and the frame members into consideration.

Tsai and Huang [15,16] numerically investigated the progressive collapse of RC frames, and examined the effects of infill walls

* Corresponding author at: Key Lab of Structures Dynamic Behavior and Control of the Ministry of Education (Harbin Institute of Technology), Harbin 150090, China.
E-mail address: shuangli@hit.edu.cn (S. Li).

http://dx.doi.org/10.1016/j.engstruct.2015.12.010
0141-0296/

on the structure's resistance capacities against progressive collapse. Their study showed that the effects largely depend on the walls' dimensions as well as their locations. They also reported that the structure's collapse resistance capacity is only slightly influenced by the infill walls, as the infill walls normally demonstrate a brittle force–displacement relationship that fails at relatively small ductility level whereas collapse of structure is a process involving exceptionally large deformation. In addition, Tsai and Huang [17] investigated the progressive collapse of RC frames with three different types of infill walls. Sasani [18] and Sasani and Sagiroglu [19] also conducted an experimental program to study this issue. In their test, they removed two adjacent columns located at the first story of an actual three dimensional, multiple spans, infilled RC frame. They showed that the Vierendeel frame action, which depicts the load redistribution following the local failure of a certain structural members, is the major collapse resisting mechanism and that the infill walls can reduce the structural deformation after the removal of columns. Nonetheless, owing to the robustness of their test frame, the structural deformation was so small that the final progressive collapse resistance capacity and damage pattern were unable to identify. In addition to the aforementioned studies on the effects of infill walls on RC frame structures, recently, similar investigations on steel frame structures with infill walls have also been executed [20–23].

All of the existing experimental studies, however, have included a complete actual frame, rather than starting with the relatively simple sub-structure (e.g., two dimensional planar frame) that consists of only the basic structural elements including the beams, columns and infill walls. Since in those studies (i.e., actual frame tests), multiple factors may affect the overall performance of the structures, it is difficult to distinguish the influences of infill walls from the influences of the other factors on the structural response. Therefore, the load transfer and redistribution between the frame members and the infill walls may not be effectively studied or understood in those kinds of experimental programs. To eliminate the disturbances caused by the other irrelevant factors, recently, Stinger and Orton [2] experimentally studied the effects of infill walls using a 1/3 scaled RC frame sub-structure specimen. Nevertheless, because the percentage of opening in the infill wall was too high (that is, the height of infill wall in their specimens was merely approximately 1/3 times that of the column), the effects of the infill walls require deeper investigations with a specific focus on different parameters, such as the other opening percentage over the infill panel area.

In a quick summary, at the present time, the laboratory experiments in the literature provide very limited data for determining the failure mechanism of structural progressive collapse and for verifying the results of numerical simulation methods for infilled RC frame structures. This study aims to experimentally evaluate the resistance capacities of two four-bay, two-story RC frame specimens, featured without and with the infill walls, against progressive collapse and to study the role that the infill walls played in the progressive failure process of the RC frames.

2. Experimental procedure

3-D frame model is widely used to address three dimensional effects such as the contribution of slabs [24,25], whereas 2-D frame model may yield conservative results if these effects are not accounted for. However, as the behaviors of infill walls mainly relate to the planer frames response with respect to progressive collapse, 2-D frame specimens are recognized accurate to represent the effects of infill walls and adopted in this study.

2.1. Specimen design

The test prototype frames were designed following the Chinese building codes [26,27], representing the typical RC frame structure in China. The first and the second stories of the prototype frame were 4.2 m and 3.3 m high, respectively. The center-to-center distance between adjacent columns was 5.1 m. The test frame specimens were 1/3 scaled, four-bay, two-story planar frames.

The geometry and reinforcement details of the two test specimens are given in Fig. 1. The design of the beams and columns in the two test specimens was identical. The difference between the two specimens was that in the first specimen there were no infill walls, while in the second the frame was infilled with walls with openings reserved for normal size windows. The left hand side (bays A and B) of Fig. 1 illustrates the geometry of the bare frame; that of the infilled frame is displayed on the right hand side (bays C and D). The center column in the first story was not presented in the structural design, to simulate the scenario of removal of column from the system due to accidental loads. Stirrups had 135 degree end hooks. Stirrups with a diameter of 4 mm were used in the end regions of the beams (within 250 mm measured from the beam end) at the spacing of 33 mm and in the middle regions of beams at the spacing of 67 mm. Stirrups with a diameter of 4 mm were used in the first story, at the spacing of 33 mm in the bottom regions of columns (within 450 mm measured from the column end) and 50 mm in other regions. The 8 mm (in diameter) stirrups at the spacing of 60 mm were used in the foundation beams. To improve the connectivity of the infill walls to the frame members, the 2 mm (in diameter) tie rebars with length 273 mm or 341 mm were used to tie the infill walls to the columns in the second story for the infilled frame [28]. The dimension of the masonry blocks were 130 mm × 63.5 mm × 63.5 mm. The average thicknesses of the horizontal and the vertical mortar joints were 8.9 mm and 5.8 mm, respectively. To mimic the practical construction sequence and schedule, the specimens were cast at three different times, for construction of the foundation, first story and second story, respectively. All of the beams and columns had a clear concrete cover of 15 mm. The material properties of the concrete, infill walls and rebars are given in Table 1.

2.2. Test setup

If a column is suddenly removed from a RC frame structure as a consequence of an accidental load, the beam–column join at the top will start to move downward. In this test program, the progressive collapse scenario was simulated by applying quasi-static loading on the center column of each specimen. Fig. 2 shows the loading and measuring systems of the test. A hydraulic jack was placed at the top of the center column to apply a vertical load, enforcing the downward displacement at the joint. A hand jack, placed at the bottom of the center column, was unloaded step by step to perform the test under displacement control. The loading method is equivalent to the well-known local push-down analyses [3]. As the test specimens were two directional planar frames, to prevent the undesired out-of-plane deformation and failure, two horizontal collar devices, each of which consisted of a pair of rollers installed on the lateral braces and arranged in the opposite directions out of the plane of frame specimen, were attached to both sides of the center column to prevent out-of-plane displacement. Similarly, four vertical collar devices installed on the lateral braces were attached to the two sides of the adjacent (to the center column) and external columns. There were 5 mm gaps left intentionally between the rollers and the column surfaces at the initial stage, to avoid unwanted frictional forces acting on the columns in the early stages of the tests.

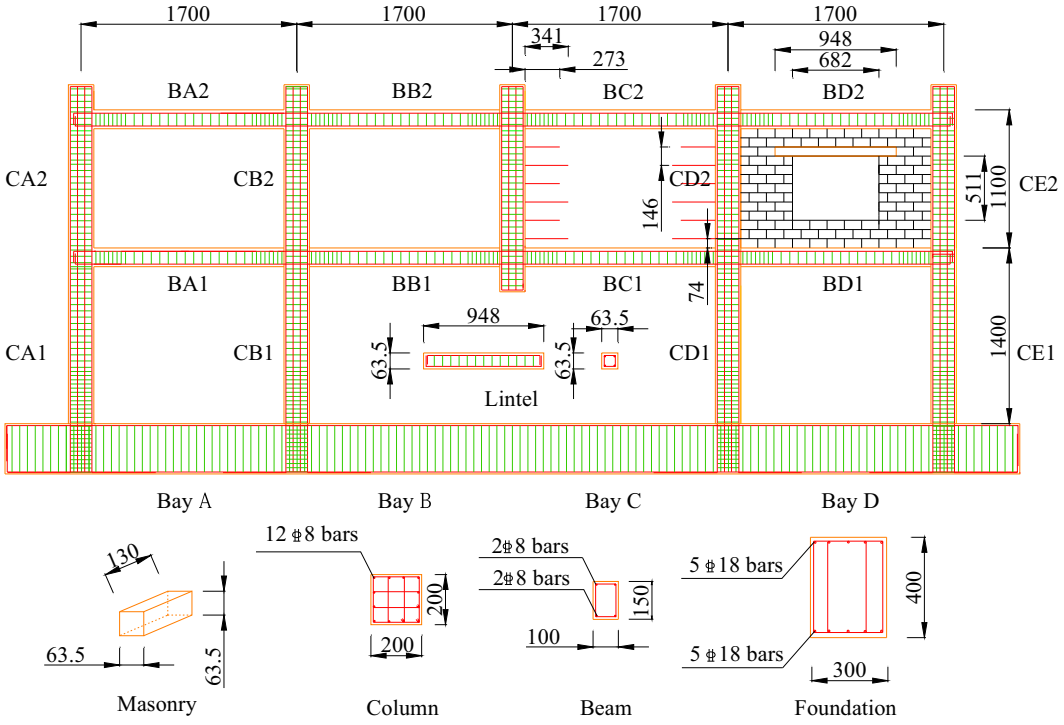

Fig. 1. Design details of test frame specimens (Bays A and B illustrate the case without infill walls; Bay C illustrates tie rebars between columns and infill walls; and bay D illustrates the case with infill walls. Unit: mm).

Table 1
Material properties of the specimens.

Concrete	Compressive strength	Foundation: 35.8 MPa First story: 41.3 MPa Second story: 31.8 MPa
Masonry	Compressive strength	22.6 MPa
Mortar	Compressive strength	18.3 MPa
Masonry unit (combination of masonry and mortar)	Compressive strength	12.8 MPa
	Shear strength	1.08 MPa
18 mm diameter rebar	Yield strength Ultimate strength Strain at fracture	338 MPa 487 MPa 0.19
8 mm diameter rebar	Yield strength Ultimate strength Strain at fracture	415 MPa 588 MPa 0.18
4 mm diameter stirrup	Yield strength Ultimate strength Strain at fracture	235 MPa 322 MPa 0.31
2 mm diameter tie rebar	Yield strength Ultimate strength Strain at fracture	339 MPa 395 MPa 0.28

As shown in Fig. 3, the instrumentation of the test frame specimens included two load cells, installed above and below the center column, to measure the applied vertical load. The difference between the forces acting at the top and bottom load cells represents the external vertical load applied on the beam–column joint. This force is equal to the resistance force provided by the test specimen against progressive collapse, i.e., the resistance force comes from the center column. Two vertical linear variable differential transformers (LVDTs) and two relative displacement meters were installed above the center column to measure the vertical displacement of the center column. Horizontal LVDTs were placed at each joint of the specimens to measure the horizontal movements of the adjacent and external columns. Strain gages attached to the rebars were installed at the two ends and mid-span of beam BC1 and at the bottom of column CD1.

3. Experimental results and discussion

The experimental results and observation of the two specimens are demonstrated with resistance and displacement, crack development and rebar fracture, and strain variation in this section. It shows that the progressive collapse process can be classified into three primary stages for both specimens, including initial stage, compressive stage, and catenary stage. As illustrated in Fig. 4, section OA refers to the initial stage characterized with basically elastic behaviors. Section AB can be considered as compressive stage, in which the bars yielding and formation of plastic hinge at the end of the deformed region of beams. According to theoretical prediction [5], the yield moment of the beams of the test specimens is 4.36 kN m, corresponding to the resistance force of the bare frame 23.25 kN. The compressive arch action contributes to the resistance in this stage. Section BC is the catenary stage, featured by the catenary action forms in beams. It starts as the strain in the bars at the original compressive region in the beams switched from compression to tension [5]. It is interesting to note that around the starting point of the catenary stage (point B), the surrounding columns changed their movements from outward to inward and moved back to their initial positions (with a horizontal displacement of 0 mm). This stage starts at the vertical displacement of center column of 204.5 mm for the bare frame and 215.5 mm for the infilled frame. The infill walls contribute to the resistance of the infilled frame throughout the three stages.

Fig. 2. Specimen loading and measuring systems (using the infilled frame as the example).

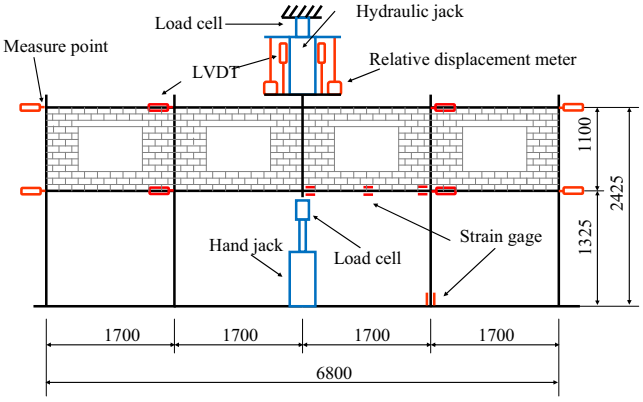

Fig. 3. Test instrumentations (using the infilled frame as the example. Unit: mm).

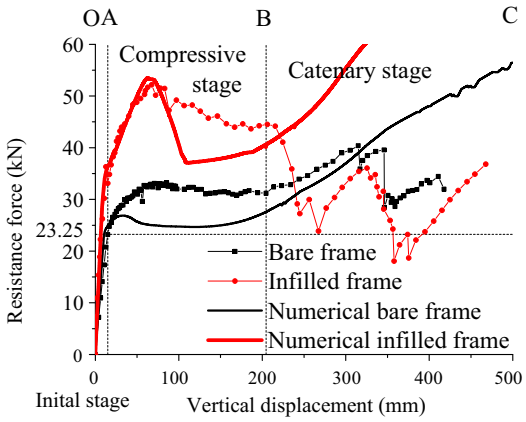

Fig. 4. Resistance force versus vertical displacement of the central column for the frames.

3.1. Resistance and displacement

3.1.1. Bare frame

Fig. 4 shows the resistance force versus the vertical displacement of the center column for the bare frame. At the vertical displacement of 85.4 mm, the resistance force achieved its maximum value of 33.2 kN in the compressive stage, then gradually decreased to 31.2 kN until the end of the compressive stage (the vertical displacement of 204.5 mm). Thereafter, because of the development of catenary action in the damaged structure, the resistance force increased again in the catenary stage until the end of test, in spite of several drops in its magnitude due to rebar fractures. The test ended when the center column attained the vertical displacement of 417.7 mm. Fig. 5 shows the horizontal displacements of joints at the adjacent and external columns (see Fig. 3, the locations of LVDTs) versus the vertical displacement of the center column. According to the recorded data as reported in Fig. 5, when the vertical displacement increased in the initial stage and compressive stage, the adjacent and the external joints firstly moved outward (i.e., horizontally away from the center column) and achieved their maximum values of approximately 3.8 mm at the vertical displacement of 106.6 mm. Next, these joints moved back to their initial positions (with a horizontal displacement of 0 mm) at the vertical displacements of approximately 204.5 mm. Thereafter, the joints continued to move inward until the end of test in the catenary stage. In the initial stage and compressive stage, the horizontal displacements of joints at the first and second stories were almost the same; in the catenary stage, the horizontal displacements of joints at the second story gradually exceeded those at the first story. At the end of the test, the average inward displacement of joints at the first story and the second story was 20.8 mm and 35.1 mm, respectively, and the latter was about 1.69 times the former.

3.1.2. Infilled frame

Fig. 4 also shows the resistance force versus the vertical displacement of the center column for the infilled frame. From the vertical displacement of 12.8 mm to 14.9 mm, a drop in resistance force was occurred because of the cracks in the infill walls. It should be note that 14.9 mm is also assigned to the end of the initial stage for both of the frame specimens, because as for the bare frame, the vertical displacement about 14.9 mm corresponds to the formation of plastic hinges in beams by theoretical prediction. At the vertical displacement of 67.5 mm, the resistance force achieved its maximum value of 52.2 kN, then gradually decreased to 41.1 kN until the vertical displacement reached 224.5 mm. After that point, the resistance force dropped several times due to rebar fractures before it increased again owing to the catenary action. The test ended at the vertical displacement of 467.7 mm. Fig. 6 shows the horizontal displacements of joints at the adjacent and external columns versus the vertical displacement of the center column. Similar to the response of the bare frame, as the vertical displace-

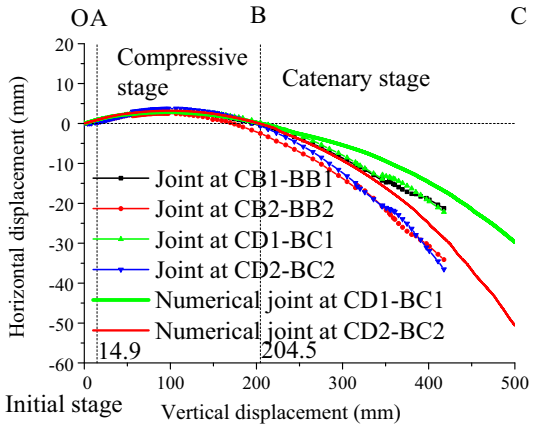

(a) Adjacent columns

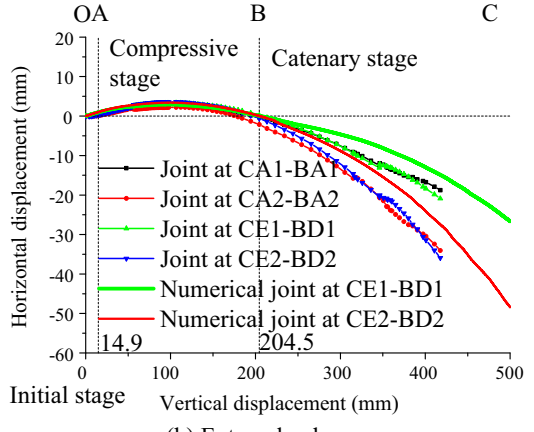

(b) External columns

Fig. 5. Horizontal displacements of joints versus vertical displacement of the central column for the bare frame.

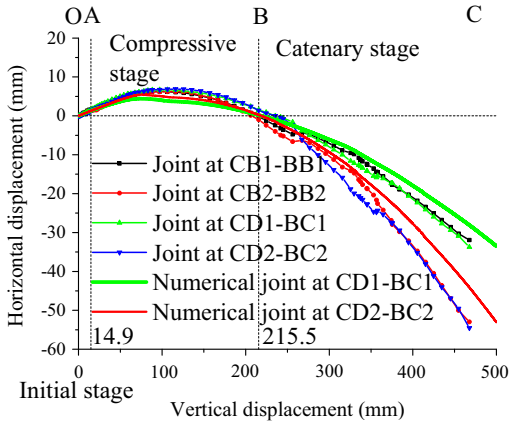

(a) Adjacent columns

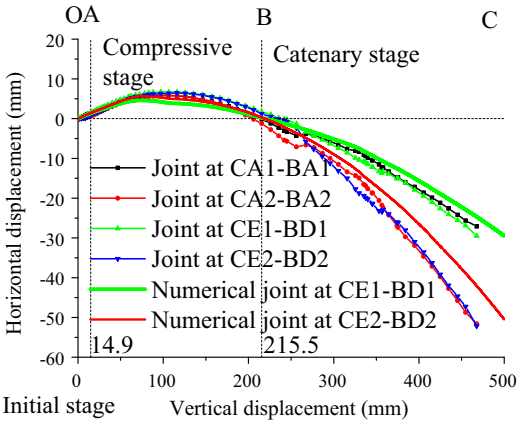

(b) External columns

Fig. 6. Horizontal displacements of joints versus vertical displacement of the central column for the infilled frame.

ment increased, the adjacent and external joints firstly moved outward and achieved their maximum values of approximately 6.8 mm at the vertical displacement of 106.3 mm. Then, the joints moved back to their initial positions (with a horizontal displacement of 0 mm) at the vertical displacements of approximately 215.5 mm (the end of the compressive stage and the start of catenary stage). Thereafter, the joints continued to move inward until the end of test. In the compressive stage, the horizontal displacements of joints at the first and second stories were almost the same, but in the catenary stage, the horizontal displacements of joints at the second story gradually exceeded those at the first story. At the vertical displacement of 415.3 mm, approximately at which point the test for the bare frame ended, the average inward displacement of joints at the first story and second story was 22.1 mm and 37.3 mm, respectively, and the latter was about 1.69 times the former. The maximum outward horizontal displacements of the adjacent and external joints were observed to be approximately 1.79 times those of the bare frame, whereas the maximum inward horizontal displacements of joints were only approximately 1.06 times those of the bare frame when compared at the vertical displacement of 417.7 mm.

3.2. Crack development and rebar fracture

3.2.1. Bare frame

Fig. 7 shows the crack propagation observed at three stages of the test. In the end of initial stage, (the vertical displacement of 14.9 mm), only three or four cracks emerged at the ends of beams in bays B and C. At the maximum compressive stage (the vertical displacement of 85.4 mm), the major cracks, which formed in beams in bays B and C, further developed, but they still concentrated in regions near the beam ends. These cracks continued to widen and extend until the end of the compressive stage. (the vertical displacement of 204.5 mm). In the compressive stage, the cracks in the beams were mainly caused by the bending moment, which achieved their maximums at the beam end cross-sections. In the catenary stage, due to the gradually increasing inward horizontal displacements of joints, new cracks began to form in regions near the beam ends in bays A and D. When the vertical displacement reached 317.1 mm, old cracks continually widened and some new cracks emerged and approached the middle of beams BB1 and BC1. After the vertical displacement reached 317.1 mm, rebars began to fracture. The two rebars in the top of left end of beam BB2 fractured at the vertical displacements of 317.1 mm and 346.3 mm, respectively, resulting in the two sharp drops in the resistance force as shown in Fig. 4. Both rebars in the top of right end of beam BC2 fractured at the vertical displacement of 354.4 mm. Since the fractures in the rebars in beams BB2 and BC2 had released the tensile forces in these beams, few new cracks formed in beams BB2 and BC2 throughout the remaining of the test. The two rebars in the bottom of left end of beam BC1 fractured at the vertical displacements of 354.4 mm and 359.0 mm, respectively. Due to the catenary action and the relative displacement between the joints at the first and the second stories, bays A and D had a horizontal deformation. The cracks in the beams in bays A and D at the vertical displacement of 417.7 mm, the end of the

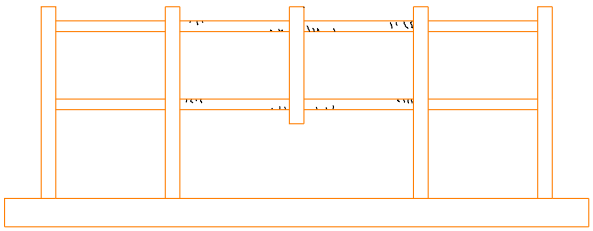

(a) At the vertical displacement of 14.9 mm (maximum initial stage)

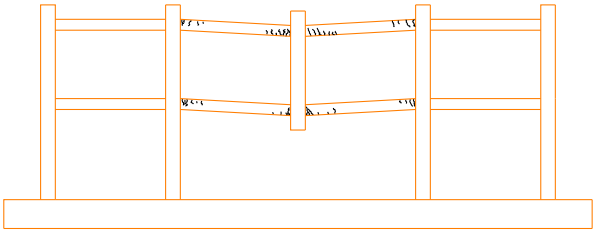

(b) At the vertical displacement of 85.4 mm (maximum compressive stage)

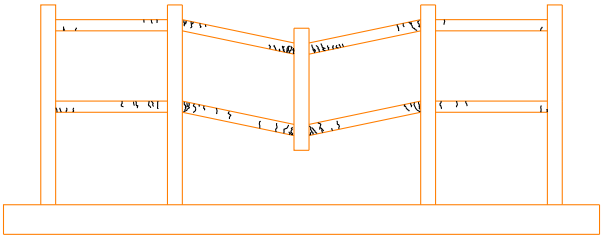

(c) At the vertical displacement of 315.0 mm (maximum catenary stage)

Fig. 7. Crack developments of the bare frame in typical deformation states.

(a) Bay A (b) Bay D

Fig. 8. Cracks in bays A and D of the bare frame at the vertical displacement of 417.7 mm, the end of the test.

test, are shown in Fig. 8. It is seen that there were only slight cracks in those beams. The final failure mode of the bare frame at the end of test is shown in Fig. 9, in which the damage was mostly concentrated in the beam ends in bays B and C, while the damage to beams in bays A and D was slight.

3.2.2. Infilled frame

The existence of infill walls changed the crack formation process. Compared with the bare frame, it is noticed that more cracks formed in the beams in the initial stage of the test and there were major cracks in the infill walls. In the end of initial stage, at a very small vertical displacement of 14.9 mm, the major cracks in the infill walls had already formed, and gradually widened in the later stages. However, after the formation of the major cracks, only a few secondary cracks gradually formed in the weak positions around the major cracks in the infill walls with the increase of the vertical displacement. Fig. 10 shows the major cracks formed in infill walls and beams at the vertical displacement of 14.9 mm, 67.5 mm and 215.5 mm, corresponding to the end of the initial stage, maximum compressive stage and maximum catenary stage. The cracks divided the infill wall into four main parts around the opening, which can be seen as four equivalent compressive struts bracing in bays B and C. The cracks in the beams were concentrated in the beam ends and in the regions near the corners of the openings. At the vertical displacements of 235.3 mm, 241.9 mm, 245.0 mm, and 267.3 mm, the rebars in the bottom of left end of beam BC2, the top of right end of beam BC1, the bottom of right end of beam BB2, and the bottom of right region of beam BB1 fractured, succes-

Fig. 9. Failure mode of the bare frame at the end of the test.

sively. As the vertical displacements increasing from 329.7 mm to 357.9 mm, the rebars in the top of left end of beam BB1, the top of left region of beam BB2, the top of right region of beam BC2, and the bottom of left region of beam BC1 fractured, successively. At the vertical displacement of 375.4 mm, one rebar in the top of left region of beam BC1 fractured. The cracks in the infill walls and beams in bays A and D at the vertical displacement of 415.3 mm, approximately corresponding to the end of the test of bare frame, are shown in Fig. 11. Unlike in the case of bare frame, in which the beams were only slightly damaged, there were many cracks found in the beams in bays A and D of this specimen. The difference of adjacent bays deformations between the two frame specimens are not too much during the catenary stage. On the other hand, the stiffness of the infilled frame in bays A and D is much higher due to the contribution of infill walls. Therefore, it can be concluded that the internal forces in the beams in bays A and D of the infilled frame are much higher than those of the bare frame, hence more cracks are distributed in the beams of the infilled frame. The final failure mode of the infilled frame at the end of the test is shown in Fig. 12, the damage of which was very different to that inflicted on the bare frame. The failure positions in the beams were located at the ends of the beams in the diagonal compression direction and nearby the corners of openings in the diagonal tensional direction.

3.3. Strain variation

3.3.1. Bare frame

Fig. 13a shows the strain variations of rebars in beam BC1 for the bare frame. It is observed that the rebars in the bottom of left

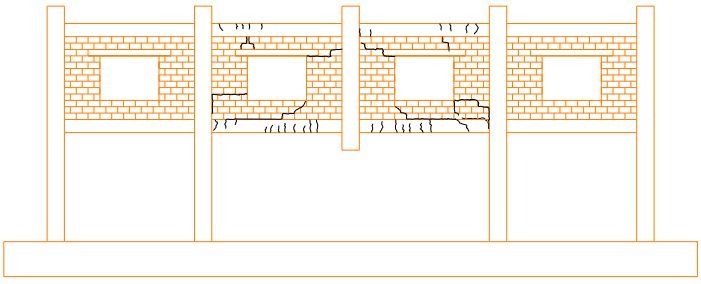

(a) At the vertical displacement of 14.9 mm (maximum initial stage)

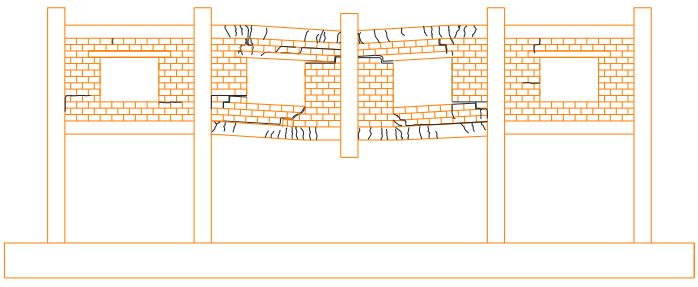

(b) At the vertical displacement of 67.5 mm (maximum compressive stage)

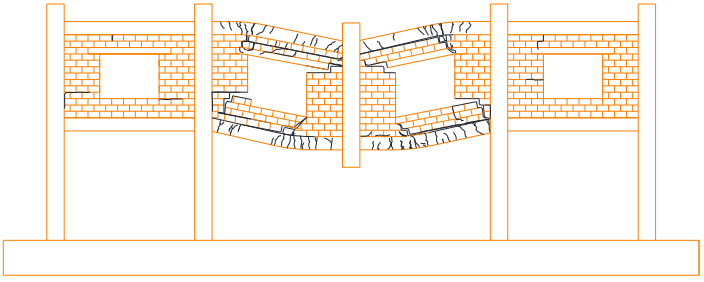

(c) At the vertical displacement of 215.5 mm (maximum catenary stage)

Fig. 10. Crack developments of the infilled frame in typical deformation states.

(a) Bay A (b) Bay D

Fig. 11. Cracks in bays A and D of the infilled frame at the vertical displacement of 415.3 mm, approximately the end of the test for the bare frame.

Fig. 12. Failure mode of the infilled frame at the end of the test.

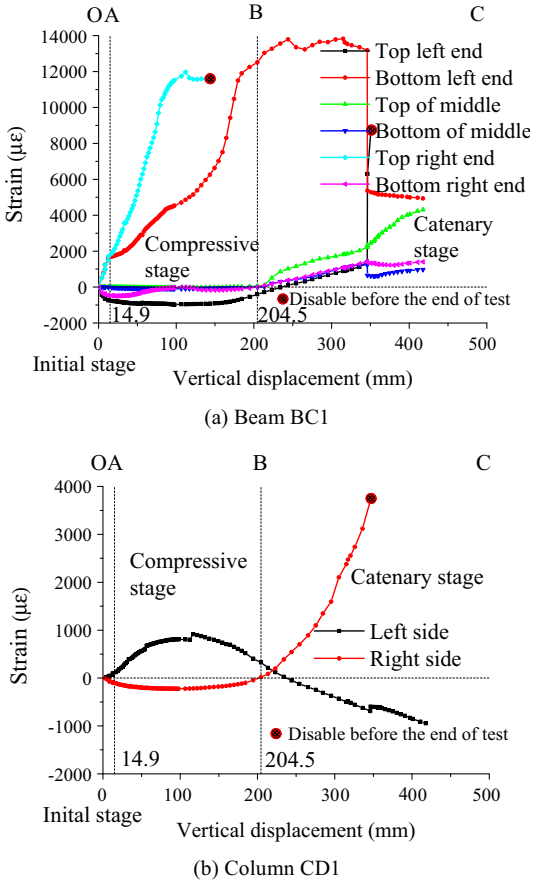

Fig. 13. Strains of rebars in beam and column for the bare frame.

end of the beam and those in the top of right end of the beam were in tension during the test. On the contrary, initially, the rebars in the top of left end, bottom of right end and in the middle of beam were in compression in the initial and compressive stages. When the vertical displacement reached 204.5 mm (the beginning of catenary stage), the strains in these rebars gradually changed from compression to tension due to the development of catenary action. After the vertical displacement of 346.3 mm, the stress in rebars in the bottom of left end sharply dropped because of rebar fracture processes. Meanwhile, the stress in rebars in the top of left end considerably increased because the tension forces were transferred from the fractured rebars to un-fractured ones. Fig. 13b shows the strain variations of rebars in the bottom end of column CD1. It can be observed that in compressive stage, the left side in the bottom end of column CD1 was in tension and the right side was in compression. In the catenary stage, the left side shifted into compression and the right side into tension. This reconfirmed the change of direction of the joint's movement from outward to inward during the test.

3.3.2. Infilled frame

Fig. 14a shows the strain variations of the rebars in beam BC1 for the infilled frame. It is seen that the rebars in the bottom of middle of beam were in tension during the test. The rebars in the top of middle and bottom of right end changed from compression into tension due to the occurrence of catenary action. Unlike the strains in the bare frame, strains were concentrated in the right part of beam BC1, and strains in the left end of beam BC1 were small during the whole test. This proved that the load distribution was changed in the infilled frame and the deformation of beam BC1 was concentrated in the right part due to the contribution of equivalent compressive strut mechanism. The phenomena will be further discussed in the later Section 3.4.2. Fig. 14b shows the strain variations of the rebars in the bottom end of column CD1. It can be observed that at the beginning of test, the left side in the bottom end of CD1 was in tension and the right side was in compression. Later, due to the catenary action, the left side shifted into compression and the right side into tension.

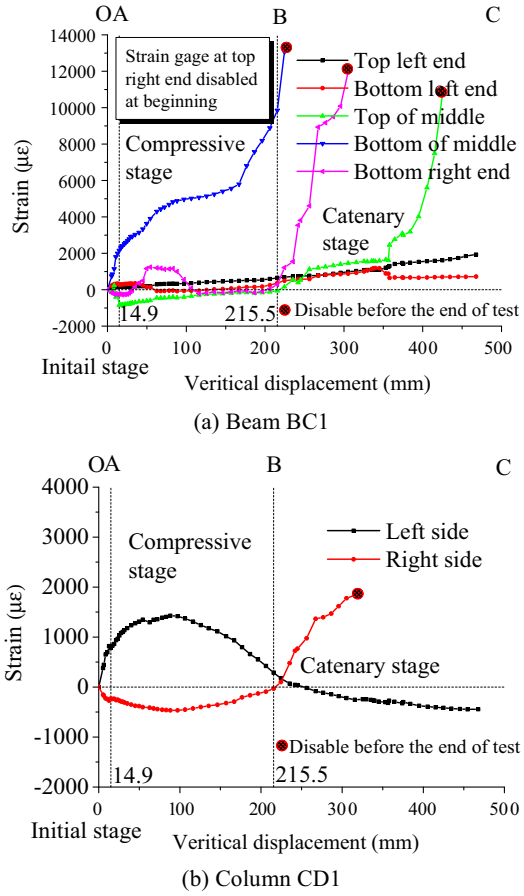

Fig. 14. Strains of rebars in beam and column for the infilled frame.

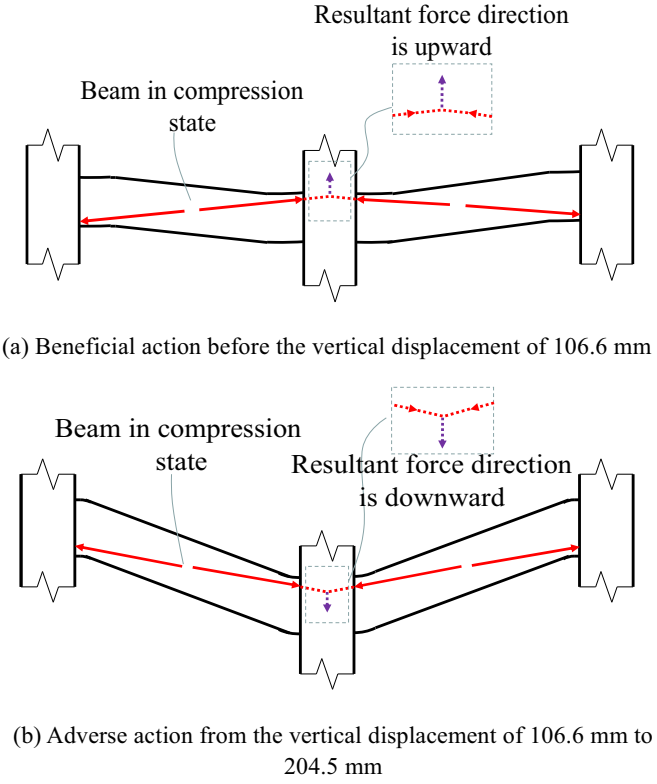

Fig. 15. Schematic diagram of beneficial and adverse compressive arch actions to resistance force.

3.4. Failure mechanism

3.4.1. Bare frame

As previously mentioned, the progressive collapse process can be classified into three stages, including the initial stage, compressive stage and the catenary stage. In the compressive stage, the compressive arch action is activated and contributes to the resistance force. It is very easy to note that the length of the line connecting two diagonal corners of the beam exceeds the horizontal length of the beam in the centroidal axis. When the center column was pushed downward, the originally inclined diagonal line will gradually move into the horizontal position. Consequently, the adjacent and external joints will be pushed outward. As the outward movement of the joints is restrained by the lateral stiffness of the columns, the compressive arch action is triggered. Intuitively, the maximum resistant force value was expected at a vertical displacement of 106.6 mm by when the joints attained their maximum horizontal outward displacements. It was observed, however, that the resistance force reached its maximum at the vertical displacement of 85.4 mm, instead. This was because the vertical components of the forces resulted from the compressive arch action decreased, despite the compressive forces in beams being kept increasing, as the originally inclined diagonal line became horizontal as the vertical displacement varied from 85.4 mm to 106.6 mm. After the vertical displacement reached 106.6 mm, the compressive forces in beams started to decrease because the diagonal line became inclined again from that moment and the compressive arch action gradually transited into the catenary action, as illustrated in Fig. 15.

The maximum horizontal outward displacements of joints occurred at the vertical displacement of 106.6 mm, implying that the direction of the compressive forces in beams was nearly horizontal at this deformed configuration. Therefore, the compressive arch action was unstable at this condition, and it was adverse to the load resistance capacity of the joint when the vertical displacement increased from 106.6 mm to 204.5 mm. The adverse effect can be explained by the schematic diagram shown in Fig. 15. Before the vertical displacement reached 204.5 mm, the beams were always in compression and the joints always moved outward. However, at the vertical displacement of 106.6 mm, the directions of the vertical components of the compressive forces in the beams began to shift from pointing upward to downward, which imposed an additional load on the center column, implying the transition from beneficial compressive arch action to the adverse compressive action. These explain the gradually decrease in resistance force as the vertical displacements increasing from 85.4 mm to 204.5 mm.

3.4.2. Infilled frame

As illustrated in Fig. 16, the infill walls in the bays bridging the center column (i.e., bays B and C) can be seen as four equivalent compressive struts, and each strut provided an alternative path for load transfer. One portion of load on the center column transferred from beams BB2 and BC2 and then through struts 3 to adjacent bays, and another portion of load transferred from struts 4 and then through beams BB1 and BC1 to adjacent bays. Load was transferred to the adjacent resisting elements thanks to the axial and flexural stiffness of the beams, and to the compressive actions in the struts. Because of the alternative load paths, unlike the bare frame, relative small portion of load was transferred in the beams at the region above the struts 3 and below the struts 4. These explain the different failure modes and different strains development in beam BC1 between the infilled frame and bare frame.

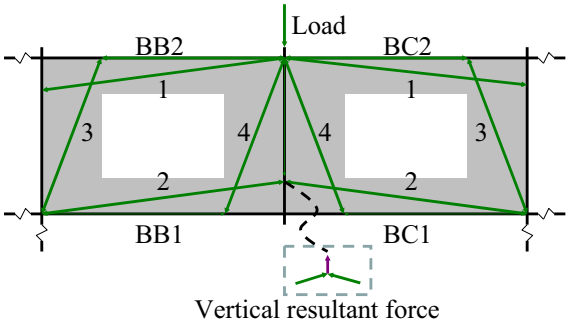

(a) At the initial stage

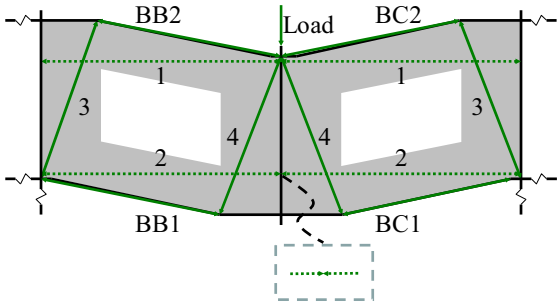

(b) The invalidation of load paths 1 and 2 at the vertical displacement of 224.5 mm

Fig. 16. Alternative load paths in bays B and C for the frame with infill walls.

The other portion of load on the center column was transferred through struts 1 and 2 to the adjacent bays by the form of axial compressive force. Because of the cracks development and the change of direction of the struts 1 and 2, the effects of struts 1 and 2 reduced as the vertical displacement increased. These explain the resistance force decreasing from the vertical displacement of 67.5 mm to 224.5 mm.

3.5. Comparison of the two specimens

The progressive collapse processes of both the specimens before the final failures demonstrated three loading stages. In the first stage, the bending capacities of the beams provided the resistance force; in the second stage, the bending capacities and compressive arch action of the beams provided the resistance force; in the third stage, the tensile forces of the rebars in the beams begin to provide the resistance force, i.e., the catenary action. The infill walls served as compressive struts and contributed to the resistance force throughout the three stages. The joints moved outward horizontally and then moved inward, and the joint displacements at the second story gradually exceeded those at the first story as the vertical displacement of the center column increased. The existence of infill walls changed the rebar strain distribution in the beams, but had little influence on the rebar strain distribution in the columns. Furthermore, the existence of infill walls changed the load transfer path and failure mode of the frames.

The infilled frame provided a larger initial secant stiffness. Through a comparison of the initial secant stiffness calculated based on 10–50% maximum resistance forces of both the specimens in the initial stage, as shown in Table 2, it can be found that the ratio of the initial secant stiffness between the infilled frame and the bare frame was 1.62.

In the compressive stage, the maximum resistance forces of the bare frame and the infilled frame occurred at the vertical displacements of 85.4 mm and 67.5 mm, respectively. As shown in Table 2, the maximum resistance force of the infilled frame was 1.57 times that of the bare frame. The infilled frame had a larger outward horizontal displacement of joint. The vertical displacements of the center column corresponding to the maximum outward horizontal displacement of joint of the both specimens were 106.6 mm and 106.3 mm, respectively. The catenary stage started at the vertical displacement of 204.5 mm and 215.5 mm for the bare frame and infilled frame, respectively.

The reason for the first significant drop in the resistance force of the bare frame and the infilled frame was the bending failures of beams induced by fractures of the rebars. As shown in Table 2, the vertical displacements corresponding to the first rebar fracture in the two specimens were 317.1 mm and 235.3 mm, respectively. Therefore, infill walls reduced the ductility performance of the frame. It was observed from Fig. 4, after the first fracture of the rebar, which happened at the vertical displacement of 235.3 mm, the resistance force of the infilled frame was close to or even lower than that of the bare frame.

4. Macro modeling

Macro finite element model analysis conducted by OpenSees [29] was performed to investigate the behavior of the test frame specimens. Parametric analyses were carried out to further study the sensitivity of the infill wall to the resistance force of the infilled frame. The center column was pushed down controlled by displacement to mimic loading strategy in this test.

Beams and columns were modeled using force-based beam–column elements, with five integration points along each element length and Corotational coordinate transformation for geometric nonlinearity. Three layers of fibers in the cover region and twenty layers of fibers in the core region were assigned to model the beam and column cross-sections. Rebar materials were modeled by using bilinear material model, with elastic modulus 2.0×10^5 MPa and strain hardening 0.5%. Concrete materials were assumed by using Kent–Scott–Park model [30,31], with material properties specified in Table 3 according to the test. Infill walls were seemed as four solid infill region surrounding the opening and each region was modeled as a pair of diagonal equivalent compressive struts (only the compressive strut is effective) using truss element as illustrated in Fig. 17. According to [15,16], the strut width a for each solid infill region in progressive collapse scenario are estimated and modified as

Table 2
Comparison of the test results.

	Secant stiffness in initial stage (kN/mm)	Maximum resistance force at compressive stage (kN)	Vertical displacement when joints achieved outward maximum displacement at compressive stage (mm)	Beginning of the catenary stage	Vertical displacement at the first bar fracture
Bare frame	1.57 (1.00)	33.2 (1.00)	106.6 (1.00)	204.5 (1.00)	317.1 (1.00)
Infilled frame	2.55 (1.62)	52.2 (1.57)	106.3 (1.00)	215.5 (1.05)	235.3 (0.74)

Note: (·) denotes ratio to values for the bare frame.

Table 3
Material parameters used in Opensees' Kent–Scott–Park model.

		Maximum compressive strength f_c (MPa)	Strain at maximum strength ε_c	Crushing strength f_{cu} (MPa)	Strain at crushing strength ε_{c2}
Cover concrete	1st story	41.3	0.002	8.26	0.006
	2nd story	31.8	0.002	6.36	0.006
Confined concrete	1st story beam	45.2	0.0022	9.04	0.016
	1st story column	44.0	0.0021	8.80	0.012
	2nd story beam	35.7	0.0022	7.14	0.016
	2nd story column	34.5	0.0022	6.90	0.012
Struts	1, 1′ and 2, 2′	9.08	0.0022	0.908	0.0055
	3, 3′ and 4, 4′	12.79	0.0022	1.279	0.0055

$$a = 0.175(\lambda_1 l_b)^{-0.4} r_{\text{inf}} \tag{1}$$

in which

$$\lambda_1 = \left[\frac{E_\theta t_{\text{inf}} \sin 2\alpha}{4E_{fe} I_b L_{\text{inf}}}\right]^{\frac{1}{4}} \tag{2}$$

where l_b is the beam length between centerlines of columns or between the centerline of the column and the location taking into consideration the dimensions of the left and right infill regions; r_{inf} and t_{inf} is the diagonal length and thickness of the infill region, respectively; $\alpha = \arctan(L_{\text{inf}}/H_{\text{inf}})$; I_b is moment of inertia of beams; E_{fe} is elastic modulus of frame material; L_{inf} and H_{inf} are the length and height of the infill region, respectively; and E_θ is the elastic modulus of infill region estimated as [32]

$$E_\theta = \frac{1}{\frac{1}{E_0}\cos^4\theta + \left[-\frac{2\nu_{0-90}}{E_0} + \frac{1}{G}\right]\cos^2\theta \sin^2\theta + \frac{1}{E_{90}}\sin^4\theta} \tag{3}$$

where $\theta = \arctan(H_{\text{inf}}/L_{\text{inf}})$; ν_{0-90} is the Poisson's ratio; E_0 and E_{90} are the Young's modulus in the directions parallel and normal to the bed joints, respectively; and G is shear modulus. According to Ref. [33], $E_{90} = 900f'_{m-90}$ and $G = 0.4E_{90}$, in which f'_{m-90} is the compressive strength normal to the bed joints. According to Ref. [34], $E_0 = 0.7E_{90}$.

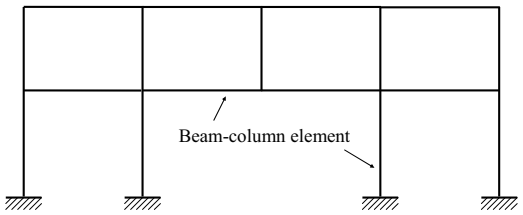

(a) Frame members in the model

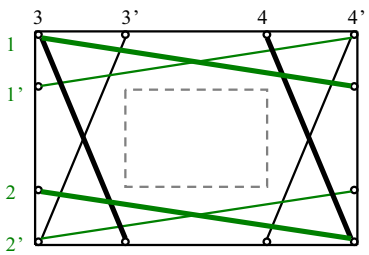

(b) Struts layout in each bay (only struts in compression are effective in the model)

Fig. 17. Macro finite element model of the test frame specimens.

a is the strut width proposed on the assumption of frame members constraining both sides of diagonal region of the infill walls. In view of the frame members constraining only one side of diagonal region of the infill region, the effective struts width of the infill region w is assumed as $a/2$. In this study, w is 77.0 mm for struts 1, 1′ and 2, 2′, 65.8 mm for struts 3, 3′ and 4, 4′.

The strut strength is estimated as $f_{m-\theta} = \frac{E_\theta}{E_{90}} f'_{m-90}$ [35]. The strut material is also assumed by Kent–Scott–Park model [30,31], According to the test results the parameters used in the model are specified in Table 3. Note that a progressive collapse analysis, only uses the monotonic curve of the Kent–Scott–Park model, rather than the hysteretic rules. Therefore, the masonry material behavior can be represented by using of a concrete material model with a reliable accuracy.

The numerical simulation results were compared with those observed from the experiment in Figs. 4–6. The numerical response gave acceptable predictions for the overall behaviors of the frame specimens. However, the numerical maximum resistance force of the bare frame was smaller than the experimental value in the compressive stage. This was in part due to that the beneficial compressive arch action cannot be represented by the macro model using beam–column elements. The compressive stress of struts 1, 2 and 3, 4 in bay C is shown in Fig. 18. Struts 3 and 4 worked during the test, whereas struts 1 and 2 failed at the peak load. The reduction of compressive force in struts 1 and 2 caused decreasing in the resistance force of the infilled frame. To further investigate the effects of struts on the progressive collapse performance of infilled frames, the models with the compressive strength of struts 1, 2 and 3, 4 scaled from 0.5 to 1.5 times were compared in Fig. 19. It can be seen that the maximum resistance force was enhanced, with increasing the compressive strength of struts 1 and 2. However, the overall behavior only has slightly change as the compressive strength of struts 3 and 4 was increased.

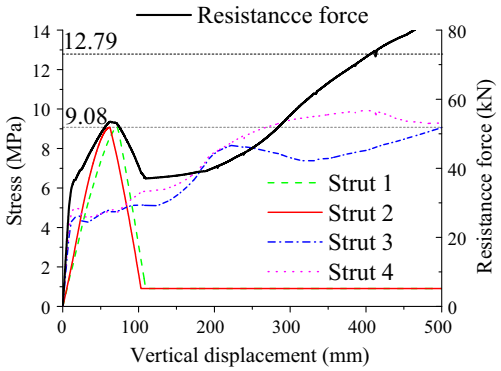

Fig. 18. Axial force of struts 1, 2, 3, and 4 in bay C.

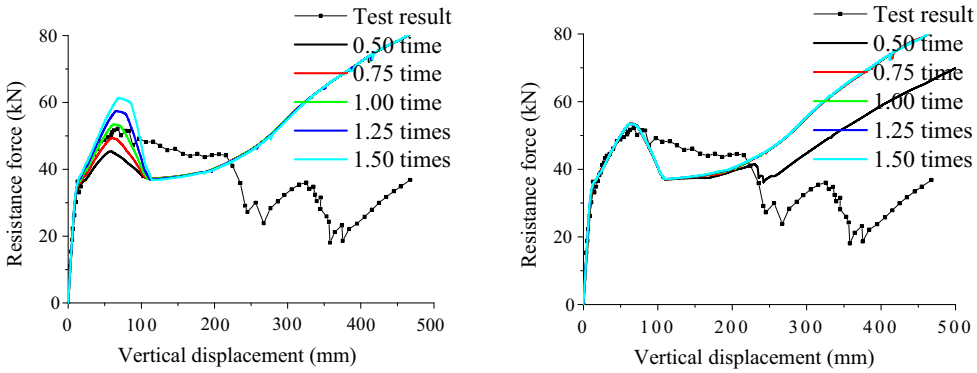

(a) Struts 1 and 2 in bay C (b) Struts 3 and 4 in bay C

Fig. 19. Influence of strut strength on the resistance force of the infilled frame.

5. Conclusions

Two four-bay, two-story RC frame specimens without infill walls and with infill walls were constructed to study the progressive collapse performance of the RC frames. The variations in the resistance force, horizontal displacement of joint, strains in the beams and columns, development of cracks in infill walls, beams and columns, rebar fractures, failure mechanisms were provided in this study. The test data supplement the existing progressive collapse tests, with an emphasis on the infill wall effects. The observations and findings drawn from the test results are summarized below.

In the compressive stage, the maximum resistance force in the case of infilled frame was larger than that in the bare frame, however, in the catenary stage, the resistance force in the former case may become smaller than the latter. The capacity of the infilled frame was dominated by the maximum resistance force in the compressive stage. Therefore, the infilled frame buildings may collapse in this stage in the real progressive collapse scenario, rather than in the catenary stage as the bare frame buildings.

Compared with the bare frame, the infilled frame has a larger initial stiffness but lower ductility. At a same vertical displacement of the center column, more damage emerged at beams in bays bridging the center column and in adjacent bays for the infilled frame. Therefore, for the case with a large external load or fragile structure to the progressive collapse, although there was a relative larger maximum resistance force, infill walls may lead to more damage to the structure. The major cracks in the infill walls and the cracks in beams formed in the early stage with a very small deformation. Also, the first fracture of rebar occurred at a smaller vertical displacement of the center column.

The maximum outward horizontal displacements of joints in the columns adjacent to the center column in the infilled frame were larger than those of the bare frame. Therefore, larger horizontal forces and more damage were developed in adjacent bays in the infilled frame in the compressive stage. Depending on the deformed configuration of the beams, the compressive arch action may induce either a beneficial or an adverse effect on the resistance force. The mechanical model of the infill wall can be seen as equivalent compressive struts which provided alternative load paths to redistribute the loads supported by the beams. Similar to the case of bare frame, the failures of beams occurred when their bending capacities were exceeded.

The experimental results were verified by the macro model proposed in this study. By modifying the compressive strength of equivalent compressive struts from 0.5 to 1.5 times of their experimental values, the results indicated that the maximum resistance force in compressive stage is greatly influenced by compressive strength of struts 1 and 2, whereas the overall behavior is slightly influenced by the compressive strength of struts 3 and 4. Due to the contribution of equivalent compressive struts, the deformed configuration was different and some failure positions of the beams were changed from the beams end to the location nearby the corners of opening. To improve the progressive collapse performance, it is an effective way for the infilled frame to strengthen the beam regions nearby the corners of the opening in engineering applications.

Acknowledgments

This research project is supported by the National Natural Science Foundation of China (Grant Nos. 51008101, 51578202, 51278150), and the China Postdoctoral Science Foundation (No. 2012T50361). The financial support of these research funds are greatly appreciated by the authors. The first author thanks for the financial support from China Scholarship Council (CSC, File No. 201306120170). The authors acknowledge the constructive comments and feedback of Prof. Halil Sezen at the Ohio State University at Columbus.

References

[1] Mohamed OA. Progressive collapse of structures: annotated bibliography and comparison of codes and standards. J Perform Constr Facilities 2006;20(4):418–25.
[2] Stinger SM, Orton SL. Experimental evaluation of disproportionate collapse resistance in reinforced concrete frames. ACI Struct J 2013;110(3):521–30.
[3] Fascetti A, Kunnath SK, Nisticò N. Robustness evaluation of RC frame buildings to progressive collapse. Eng Struct 2015;86:242–9.
[4] Su Y, Tian Y, Song X. Progressive collapse resistance of axially-restrained frame beams. ACI Struct J 2009;106(5):600–7.
[5] Yi WJ, He QF, Xiao Y, Kunnath SK. Experimental study on progressive collapse-resistant *behavior* of reinforced concrete frame structures. ACI Struct J 2008;105(4):433–9.
[6] Yu J, Tan KH. Experimental and numerical investigation on progressive collapse resistance of reinforced concrete beam column sub-assemblages. Eng Struct 2013;55:90–106.
[7] Pham XD, Tan KH. Experimental study of beam-slab substructures subjected to a penultimate-internal column loss. Eng Struct 2013;55:2–15.
[8] Bao YH, Lew HS, Kunnath SK. Modeling of reinforced concrete assemblies under column-removal scenario. J Struct Eng 2014;140(1):1–13. 04013026.
[9] Morone DJ, Sezen H. Simplified collapse analysis using data from building experiment. ACI Struct J 2014;111(4):925–34.
[10] Sasani M, Werner A, Kazemi A. Bar fracture modeling in progressive collapse analysis of reinforced concrete structures. Eng Struct 2011;33(2):401–9.
[11] Keyvani L, Sasani M, Mirzaei Y. Compressive membrane action in progressive collapse resistance of RC flat plates. Eng Struct 2014;59:554–64.

[12] Qian K, Li B. Dynamic performance of RC beam–column substructures under the scenario of loss of a corner column – experimental results. Eng Struct 2012;42(2):154–67.
[13] Qian K, Li B. Performance of three-dimensional reinforced concrete beam–column substructures under loss of a corner column scenario. J Struct Eng 2013;139:584–94.
[14] Qian K, Li B. Quantification of slab influences on the dynamic performance of RC frames against progressive collapse. J Perform Constr Facilities 2015;29(1):1–11. 04014029.
[15] Tsai MH, Huang TC. Effect of interior brick-infill partitions on the progressive collapse potential of a RC building: linear static analysis results. Int J Eng Appl Sci 2010;6(1):1–7.
[16] Tsai MH, Huang TC. Numerical investigation on the progressive collapse resistance of an RC building with brick infills under column loss. Int J Eng Appl Sci 2011;7(1):27–34.
[17] Tsai MH, Huang TC. Progressive collapse analysis of an RC building with exterior partially infilled walls. Struct Des Tall Special Build 2013;22(4):327–48.
[18] Sasani M. Response of a reinforced concrete infilled-frame structure to removal of two adjacent columns. Eng Struct 2008;30(9):2478–91.
[19] Sasani M, Sagiroglu S. Progressive collapse resistance of Hotel San Diego. J Struct Eng 2008;134(3):478–88.
[20] Kim J, Lee H. Progressive collapse-resisting capacity of framed structures with infill steel panels. J Constr Steel Res 2013;89:145–52.
[21] Farazman S, Izzuddin BA, Cormie D. Influence of unreinforced masonry infill panels on the robustness of multistory buildings. J Perform Constr Facilities 2013;27(6):673–82.
[22] Song BI, Sezen H. Experimental and analytical progressive collapse assessment of a steel frame building. Eng Struct 2013;56:664–72.
[23] Sezen H, Song BI, Giriunas KA. Progressive collapse testing and analysis of a steel frame building. J Constr Steel Res 2014;94:76–83.
[24] Li H, El-Tawil S. Three-dimensional effects and collapse resistance mechanisms in steel frame buildings. J Struct Eng 2014;140(Computational Simulation in Structural Engineering):1–11 [A4014017].
[25] Fu F. 3-D nonlinear dynamic progressive collapse analysis of multi-storey steel composite frame buildings – parametric study. Eng Struct 2010;32:3974–80.
[26] Ministry of Housing and Urban–Rural Development. Code for design of concrete structures GB50010-2010. Beijing, China; 2010.
[27] Ministry of Housing and Urban–Rural Development. Code for seismic design of building GB50011-2010. Beijing, China; 2010.
[28] Ministry of Housing and Urban–Rural Development. Code for design of masonry structures GB50003-2011. Beijing, China; 2011.
[29] Mazzoni S, McKenna F, Scott MH, Fenves GL. Open system for earthquake engineering simulation: user command-language manual. Berkeley: Pacific Earthquake Engineering Research Center, University of California; 2009.
[30] Kent DC, Park R. Flexural members with confined concrete. J Struct Div 1971;97(7):1969–90.
[31] Scott BD, Park R, Priestley MJN. Stress–strain behavior of concrete confined by overlapping hoops at low and high strain rates. ACI J 1982;79(1):13–27.
[32] Shames IH, Cozzarelli FA. Elastic and inelastic stress analysis. Englewood Cliffs, NJ: Prentice-Hall; 1992.
[33] Masonry Standards Joint Committee (MSJC). Building code requirements for masonry structures (TMS 402-11/ACI 530-11/ASCE 6-11) and specification for masonry structures (TMS 602-11/ACI 530.1-11/ASCE 5-11) and companion commentaries. Farmington Hills, MI: American Concrete Institute; Reston, VA: American Society of Civil Engineers; Longmont, CO: The Masonry Society; 2011.
[34] El-Dakhakhni WW, Elgaaly M, Hamid AA. Three-strut model for concrete masonry-infilled steel frames. J Struct Eng 2003;129(2):177–85.
[35] Saneinejad A, Hobbs B. Inelastic design of infilled frames. J Struct Eng 1995;121(4):634–50.